

Recombination and photoluminescence mechanism in hydrogenated amorphous carbon

J. Robertson

Engineering Department, Cambridge University, Cambridge, CB2 1PZ, United Kingdom

(Received 12 October 1995; revised manuscript received 27 February 1996)

The luminescence mechanism in a -C:H is described as a modification of the band tail luminescence in hydrogenated amorphous Si. The tail states of a -C:H are formed from clusters of sp^2 sites and luminescence occurs by recombination within each cluster. The paramagnetic defects are confirmed as the nonradiative recombination centers. The weaker temperature dependence of the luminescence efficiency of a -C:H than a -Si:H is attributed to its wider tails which inhibit carrier hopping. The luminescence efficiency is also quenched by narrow optical gaps, because carriers can tunnel to defects more easily in the sp^2 -rich, narrow-gap a -C:H. Defect quenching is less strong, however, because of the shorter Bohr radius of localized states in a -C:H. [S0163-1829(96)07624-2]

Hydrogenated amorphous carbon (a -C:H) can be prepared with a wide range of band gaps.¹ The narrow gap a -C:H, also known as diamondlike carbon (DLC), is used as a hard, low-friction coating material. The wide gapped, "polymeric" a -C:H has a strong room-temperature photoluminescence and is being developed as an electroluminescent material.^{2,3} It is also used as a dielectric in metal-insulator-metal switches in active matrix displays.^{4,5} There is, therefore, interest in understanding the recombination and luminescence processes in a -C:H.

Photoluminescence (PL) has been studied in a -C:H (Refs. 6–11) and in associated a -Si_{1-x}C_x:H alloys.^{12–16} PL in Si-rich a -Si_{1-x}C_x:H is basically like that in a -Si:H itself.¹³ PL arises from the radiative recombination of electrons and holes trapped in the band tail states and is described in terms of a rigid-band, one-electron model.¹⁷ PL is quenched by paramagnetic Si dangling bonds which act as nonradiative recombination centers.^{17,18} There is a sudden change in the PL behavior of C-rich alloys. PL becomes much faster, almost independent of temperature,^{14,15} and is not quenched by relatively high concentrations of paramagnetic defects. Indeed, PL efficiency correlates poorly with the paramagnetic defect densities.^{8,12,13} The appropriate model of PL in a -C:H is, therefore, unclear. Is the rigid, one-electron model valid, or is it necessary to either invoke electron-lattice coupling as in a -Se (Ref. 19) or polyacetylene,²⁰ or electron-electron interactions as in other organic polymers?²¹ Also, are the paramagnetic defects the nonradiative recombination centers? This paper aims to confirm that the rigid one-electron model accounts for PL in a -C:H and that the paramagnetic defects are the nonradiative centers.

Let us first recall that a -C:H contains both sp^3 and sp^2 sites.^{22,23} The σ bonds of sp^3 and sp^2 sites give rise to σ valence and σ^* conduction-band states, separated by a band gap of order 6 eV.²² The π and π^* states of the sp^2 sites lie within the σ – σ^* gap, and form the band edges and control the optical gap. The size of the gap depends on the configuration of the sp^2 sites. π bonding favors a pairing up and clustering of sp^2 sites in a sp^3 matrix. However, ion bombardment during deposition²⁴ causes a rather large disorder potential which opposes clustering. Thus, the sp^2 clusters consist of both olefinic chain and aromatic ring groups, much

smaller than originally proposed, with a typical size of $L_a \approx 3$ Å.²³ Experimentally, the optical gap of a -C(:H) can vary widely depending on the deposition conditions. Figure 1(a) compares the optical gap of a -C:H deposited by plasma-enhanced chemical-vapor deposition^{25–27} and ta -C:H, a form of a -C:H with a high fraction of sp^3 C—C bonding.²⁹ The optical gap of all types of a -C(:H) is seen to vary in a similar, regular fashion with sp^2 content z which is almost linear,

$$E_g \approx 3 - 2.5z \text{ eV.} \quad (1)$$

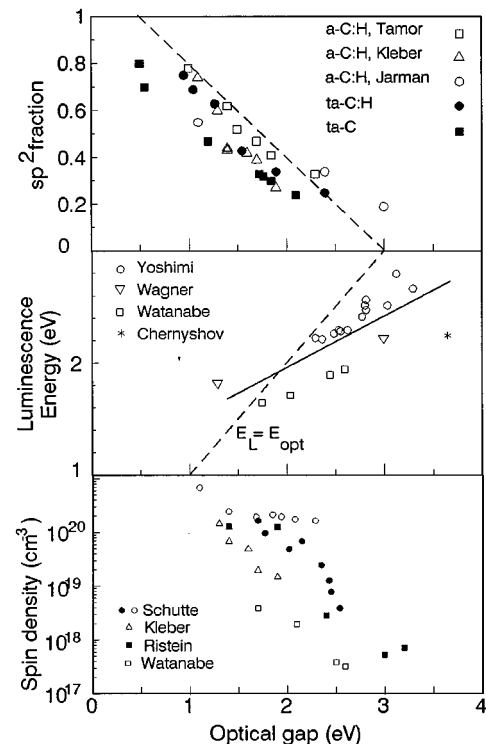


FIG. 1. (a) Variation of optical (T_{auc}) gap with sp^2 carbon fraction, as determined by electron-energy-loss spectroscopy or nuclear magnetic resonance, for PECVD a -C:H (Ref. 25–27), t a -C:H (Ref. 29), and t a -C (Ref. 28). Equation (1) is shown as a dashed line. (b) Variation of the PL energy with optical gap (Refs. 6–9 and 15). The solid line of slope 0.5 is a guide to the eye. (c) Spin density vs optical gap for a -C:H from different workers (Refs. 6, 8, 26, and 33).

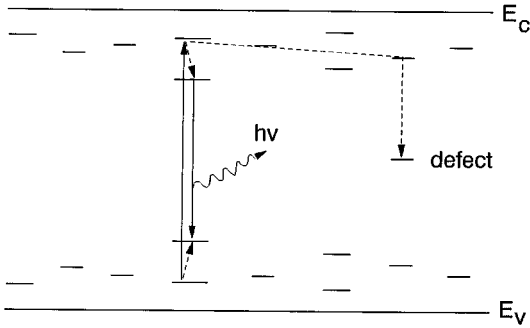


FIG. 2. Schematic band diagram of *a*-C:H showing the tail states due to sp^2 clusters. Luminescence occurs by photoexcitation and recombination in a sp^2 cluster. Nonradiative recombination occurs by the tunneling or hopping of a carrier to a defect.

This regular behavior is important and emphasizes that the sp^3 sites of *a*-C(:H) do control electronic properties such as band gap, as originally proposed.^{22,30}

The large difference of local band gaps of the sp^3 and sp^2 sites creates band-edge fluctuations, with the sp^3 sites acting as tunnel barriers between the π states of sp^2 clusters. The analysis of PL suggests that the Bohr radius of π states is about 6 Å, which is larger than the cluster size of 3 Å. The fluctuations are strong but short range, so the clusters form a single interacting system, rather than a set of weakly interacting clusters with their own internal states. It is therefore more appropriate to treat the network just like a conventional amorphous semiconductor, with disorder-induced band tails, mobility edges, and extended states (Fig. 2). The range of different cluster sizes and local gaps causes the π density of states (DOS) to tail into the gap. The π states in the tails are localized because of the low DOS, but further into the bands, at some higher DOS above a mobility edge, the states are extended. It is not clear where the mobility edges lie in *a*-C:H from experimental data, but the strength of the fluctuations may place them well above the optical band edges. Note that the fluctuations are symmetric, so that the valence and conduction tail states occur at the *same* site.³¹ These states are coupled by a large dipole matrix element, so localized to localized optical transitions are allowed in *a*-C:H. This contrasts with the usual situation, where the tail states are localized in different regions, so localized to localized transitions are forbidden.³²

Following electron hole excitation, the subsequent radiative process could, in principle, follow a number of limiting cases. If *a*-C:H behaves like a group-IV amorphous semiconductor like *a*-Si:H, the one-electron disorder potential dominates and a rigid tail state model is appropriate.

On the other hand, *a*-C:H could behave like an organic light-emitting polymer such as polyphenylvinylene (PPV). There, the electron hole interaction dominates, leading to strong excitonic features in the optical absorption and molecular behavior.²¹ However, the optical absorption spectra of *a*-C:H shows no excitonic features, indicating that disorder dominates electron-hole interactions in this system.

A high H content, luminescent *a*-C:H has a low network coordination number, and low rigidity, so lattice relaxation is easy. The electron-hole pair could become localized at a single π bond and cause it to break in a radiative or nonra-

diative transition. Such strong electron-lattice coupling, as in *a*-Se (Ref. 19) or polyacetylene,²⁰ gives a Stokes shift so the PL energy is roughly half of the optical gap. A compilation of PL data for *a*-C:H in Fig. 1(b) shows that a Stokes shift occurs, but the emission is generally well above half gap, so we believe that this polaron model is not appropriate for *a*-C:H.

We therefore consider the application of the *a*-Si:H rigid band-tail model to the PL of *a*-C:H. In *a*-Si:H, photoexcitation creates an electron-hole pair around the mobility edges. They lose energy by thermalization and fall into the tail states. Thermalization allows the spatial separation of the carriers. Luminescence occurs by tunneling recombination across the gap. Carriers which instead reach a paramagnetic defect by either hopping or tunneling will recombine nonradiatively and not contribute to PL.

In *a*-C:H, PL is fast, weakly temperature dependent, not quenched by electric fields, and shows polarization memory, indicating that the PL center is highly localized. We therefore propose that photoexcitation creates an electron-hole pair in the same cluster. The electron and hole thermalize and fall deeper into the tail states. The strong fluctuations limit their spatial separation, consistent with fast PL. PL occurs from radiative recombination, largely from carriers within the same cluster, and PL is quenched by tunneling or hopping to a nonradiative center. The basic model is therefore similar to that of *a*-Si:H, the main difference being that photoexcitation creates closely localized electron-hole pairs because of the symmetric fluctuations, and that the strength of the fluctuations keeps the pair close together until PL occurs. The idea of PL from sp^2 clusters has been proposed earlier,^{11,13,31} the present model differs in emphasizing that the small cluster size makes band-edge π states behave more like conventional tail states, rather than weakly interacting clusters with an internal electronic spectrum. We now try to show how a *a*-Si:H-type model can give a consistent account of the main features of PL such as the temperature dependence and the competition between radiative and nonradiative processes.

The degree of localization can be estimated from the PL lifetime for radiative tunneling

$$\frac{1}{\tau_r} = \frac{1}{\tau_{r0}} \exp\left(-\frac{2R}{R_0}\right), \quad (2)$$

where R is the carrier separation and R_0 is the Bohr radius of the state. τ_{r0} depends only on fundamental constants and the dipole matrix element of the transition, with $\tau_{0r} \approx 10^{-8}$ s.¹⁷ As $\tau_r \approx 10^{-8}$ s, this confirms that PL involves closely spaced carriers in the same cluster. In contrast, PL is slower in *a*-Si:H, 10^{-3} s, due to carrier separation.

The thermally activated hopping apart of carriers during thermalization causes the thermal quenching of PL. The thermal quenching can be calculated from the thermalization depth of the carriers in the band tails.¹⁷ This varies with time t as

$$E_d = kT \ln(\nu_0 t). \quad (3)$$

It is possible to define a demarkation energy E_d for the radiative lifetime $t = \tau_r$, such that carriers above E_d will hop away to defects to recombine nonradiatively, while carriers

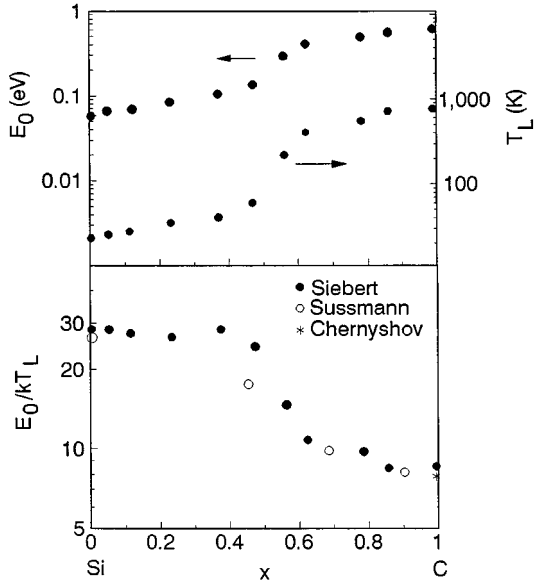


FIG. 3. (a) Variation of Urbach tail width E_0 and quenching temperature T_L with C content for $a\text{-Si}_{1-x}\text{C}_x\text{:H}$ alloys (Refs. 12 and 14–16). The T_L from Ref. 15 is used for Ref. 14 for $x=1$. (b) Variation of E_0/kT_L . Note the sudden fall in this ratio for $x>0.5$, due to the faster radiative recombination. Note also the consistency of the data from Refs. 14–16.

below E_d will remain trapped and recombine radiatively.¹⁷ We assume the band tail is described by an exponential density of states of width E_0 . The efficiency is thus the fraction of carriers trapped below E_d ,

$$\eta \approx \exp\left(-\frac{E_d}{E_0}\right) = \exp\left(-\frac{kT \ln(\nu_0 \tau_r)}{E_0}\right). \quad (4)$$

The experimental variation of the PL efficiency of $a\text{-Si:H}$ and $a\text{-C:H}$ is

$$\eta = \eta_0 \exp\left(-\frac{T}{T_L}\right). \quad (5)$$

Equation (4) has the same form if

$$kT_L = E_0 / \ln(\nu_0 \tau_r). \quad (6)$$

Equation (6) describes well the thermal quenching in $a\text{-Si:H}$ where E_0 is the width of the conduction-band tail. Equation (6) also describes thermal quenching in $a\text{-SiC:H}$ alloys, if E_0 is given by a constant fraction of the valence tail width, with this taken from the Urbach optical absorption tail. Figure 3(a) shows that the variation of characteristic temperature T_L and Urbach slope, E_0 , for $a\text{-Si}_{1-x}\text{C}_x\text{:H}$ alloys.^{8,12,14–16} E_0 and T_L are seen to increase continuously with C content and then increase sharply at $x=0.5$, consistent with the model. Figure 3(b) shows that the ratio E_0/kT_L is relatively constant for $x<0.5$, and then falls sharply at $x=0.5$ to a value of 9. This fall is due to a sharp increase in the radiative rate from τ_r 10^{-3} to 10^{-8} s,^{12,15} and is consistent with Eq. (6). It is noted that there is a common variation of the ratio E_0/kT_L for the C-rich alloys from various groups,^{14–16} despite their different band gaps. We therefore see that the existence of room temperature PL in

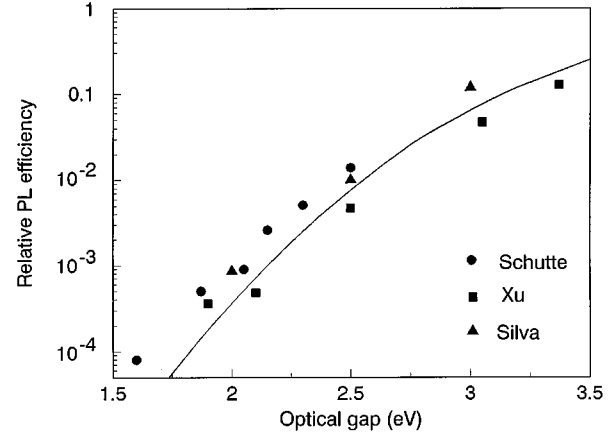


FIG. 4. Relative PL efficiency vs optical gap for the cathodic samples of Schutte (Ref. 8) Xu and Ristein (Refs. 9 and 33), and Silva (Ref. 10). The absolute efficiencies of each data set are unknown, so each was moved vertically to emphasize the common energy dependence. Values labeled Schutte are for her high defect density “cathodic” samples, the efficiencies of the “anodic” samples are similar (Ref. 8).

$a\text{-C:H}$ is fundamentally due to its 5–10 times greater tail width than $a\text{-Si:H}$. The tail width is also the cause of the wide PL band, but this and the Stokes shift between excitation and emission energy will not be covered here.

In the absence of hopping, the PL efficiency depends on the defect concentration. The electron-hole pair will recombine nonradiatively if they are formed within the tunneling capture radius R_c of a nonradiative recombination center. The relative efficiency is given by the probability of having no defects within the distance R_c ,

$$\eta = \eta_0 \exp\left(-\frac{4\pi}{3} R_c^3 N_d\right), \quad (7)$$

where N_d is the defect density.¹⁷ The capture radius R_c is defined as where the radiative and nonradiative tunneling rates are equal,

$$R_c = \frac{R_0}{2} \ln(\nu_0 \tau_r), \quad (8)$$

where τ_r is the radiative lifetime and the nonradiative lifetime for tunneling is given by

$$\frac{1}{\tau_{nr}} = \nu_0 \exp\left(-\frac{2R}{R_0}\right), \quad (9)$$

where ν_0 is the hopping attempt frequency and R_0 is the Bohr radius of the localized state.

Equations (7)–(9) describe well the defect quenching in $a\text{-Si:H}$ and Si-rich $a\text{-SiC:H}$, where N_d is identified as the density of Si dangling bonds detected by electron spin resonance.^{13,17} The correlation appears to fail for C-rich $a\text{-SiC:H}$ or $a\text{-C:H}$ (Refs. 8, 12–14) and it was concluded that paramagnetic defects were not the main nonradiative recombination center in $a\text{-C:H}$. The dominant experimental trend appears to be an exponential increase in PL efficiency with optical gap, with the *same* exponential slope, as seen in Fig. 4. The dependence on spin density is less clear cut, and in one case absent.⁸ It is nevertheless clear that PL in

a-C:H can coexist with a much higher defect density of $\approx 10^{20} \text{ cm}^{-3}$ than in *a*-Si:H. A problem in finding an underlying dependence of efficiency on spin density is that the gap and spin density tend to be correlated in *a*-C:H, as seen in Fig. 1(c).^{6,8,26,33} A second question is that the nature of the paramagnetic centers has not been settled experimentally in *a*-C because of lack of information from electron spin resonance. The defects could be either single dangling bonds or sp^2 clusters containing an odd number of sites.²² Whatever their nature, paramagnetic centers remain the best candidate for the nonradiative recombination center, because of their midgap state and their large concentrations, but the *a*-Si:H model needs to be modified.

We therefore reconsider tunneling quenching for *a*-C:H. The quenching occurs if a carrier tunnels out of the excited cluster via other clusters to a defect site where it recombines. The cluster tail states in Fig. 2 are entirely analogous to the tail states of *a*-Si:H. They decay outside the cluster with a Bohr radius, but they differ in having a finite interior size. The decay of a tail state from any cluster only occurs in the sp^3 matrix, which is a fraction $(1-z)$ of the total volume, so we must modify Eq. (7) to

$$\eta = \eta_0 \exp\left(-\frac{4\pi}{3} R_c^3 \frac{N_d}{1-z}\right). \quad (10)$$

This factor excludes the interior volume of all tail clusters from the calculation of capture radius. Note that this corrects mainly for the excluded volume of tail clusters, through

which the carriers tunnel, not for the defect center itself, so this depends little on whether the defect center is a single site (dangling bond) or a cluster. The excluded volume can be large because of the large sp^2 fraction. Equation (10) now gives a strong dependence on the optical gap because of the dependence of the gap on sp^2 content in Fig. 1(a). A further dependence on the gap may arise because R_0 and thus R_c may also depend on the gap.

Figure 4 shows that Eq. (10) can give the observed exponential dependence of PL efficiency on the band gap. Figure 4 shows a fit of (10) to the slope of the data with $E_g = 3.5 - 2.5z$ rather than (1) to allow for the wider gap, $\ln(\nu_0\tau_r) = 9$ from Eq. (9) and Fig. 3(b), R_c from Eq. (8), and with $R_0 = 5.7 \text{ \AA}$ and $N_d = 10^{20} \text{ cm}^{-3}$, each taken as constant for simplicity. Note that the Bohr radius $R_0 = 5.7 \text{ \AA}$ is much less than that of *a*-Si:H, 11 \AA , but this is only 20% less when expressed as a fraction of the respective bond lengths.

We conclude that it is possible to describe the PL of *a*-C:H broadly within the conventional model of *a*-Si:H of tail-to-tail recombination, with defects acting as the nonradiative recombination centers. The localized π states act like conventional tail states if their interior is treated as an excluded volume. The PL in *a*-C:H is faster and less temperature dependent than in *a*-Si:H because the electron-hole pair is much more localized and the PL coexists with much higher defect densities because the capture volume is much smaller, due to the smaller Bohr radius of 6 \AA compared to 11 \AA in *a*-Si:H.

- ¹J. Robertson, Prog. Solid State Chem. **21**, 199 (1991).
- ²S. M. Kim and J. F. Wager, Appl. Phys. Lett. **53**, 1880 (1988).
- ³M. Yoshimi, H. Shimizu, K. Hattori, H. Okamoto, and Y. Hamakawa, Optoelectron. **7**, 69 (1992).
- ⁴T. Mandel, M. Frischholz, R. Helbig, and A. Hammerschidt, Appl. Phys. Lett. **64**, 3637 (1994).
- ⁵E. Leuder, in *Amorphous Silicon Technology—1995*, edited by M. Hack *et al.*, MRS Symposia Proceedings No. 377 (Materials Research Society, Pittsburgh, 1995), p. 847.
- ⁶I. Watanabe, S. Hasegawa, and Y. Kurata, Jpn. J. Appl. Phys. **21**, 856 (1981).
- ⁷J. Wagner and P. Lautenschlager, J. Appl. Phys. **59**, 2044 (1986).
- ⁸S. Schutte, S. Will, H. Mell, and W. Fuhs, Diamond Related Mat. **2**, 1360 (1993).
- ⁹S. Xu, M. Hundhausen, B. Yan, and L. Ley, J. Non-Cryst. Solids **164**, 1127 (1993).
- ¹⁰S. R. P. Silva, Rusli, G. Amaratunga, J. Robertson, and J. Schwan, Philos. Mag. B (to be published).
- ¹¹F. DeMichelis, S. Schreiter, and A. Tagliaferro, Phys. Rev. B **51**, 2143 (1995).
- ¹²W. Siebert, R. Carius, W. Fuhs, and K. Jahn, Phys. Status Solidi B **140**, 311 (1987).
- ¹³S. Liedtke, K. Jahn, F. Finger, and W. Fuhs, J. Non-Cryst. Solids **97**, 1083 (1987).
- ¹⁴S. Liedtke, K. Lips, K. Jahn, and W. Fuhs, J. Non-Cryst. Solids **114**, 522 (1989).
- ¹⁵S. V. Chernsychev, E. I. Terukov, V. A. Vassilyev, and A. S. Volkov, J. Non-Cryst. Solids **134**, 218 (1991).
- ¹⁶R. S. Sussmann and R. Ogden, Philos. Mag. B **44**, 137 (1981).
- ¹⁷R. A. Street, *Hydrogenated Amorphous Silicon* (Cambridge University Press, Cambridge, 1991).
- ¹⁸R. A. Street, J. Zesch, and M. J. Thompson, Appl. Phys. Lett. **43**, 672 (1983).
- ¹⁹R. A. Street, Solid State Commun. **24**, 363 (1977).
- ²⁰W. P. Su, J. R. Schieffer, and A. J. Heeger, Phys. Rev. Lett. **44**, 1698 (1979).
- ²¹H. Bässler, M. Gailberger, R. F. Mahrt, J. M. Oberski, and G. Weiser, Synth. Met. **49-50**, 341 (1992).
- ²²J. Robertson and E. P. O'Reilly, Phys. Rev. B **35**, 2946 (1987).
- ²³J. Robertson, Diamond Related Mat. **4**, 297 (1995).
- ²⁴J. Robertson, Diamond Related Mat. **3**, 364 (1994).
- ²⁵M. A. Tamor and W. C. Vassell, J. Appl. Phys. **76**, 3823 (1994); M. A. Tamor, W. C. Vassell, and K. R. Carduner, Appl. Phys. Lett. **58**, 592 (1991).
- ²⁶R. Kleber, K. Jung, H. Ehrhardt, J. Muhling, K. Breuer, H. Melz, and F. Engelke, Thin Solid Films **205**, 274 (1991).
- ²⁷R. H. Jarman, G. J. Ray, and R. W. Stadley, Appl. Phys. Lett. **49**, 1065 (1986).
- ²⁸P. J. Fallon, V. S. Veerasamy, C. A. David, J. Robertson, G. Amaratunga, W. I. Milne, and J. Koskinen, Phys. Rev. B **48**, 4777 (1993).
- ²⁹M. Weiler, S. Sattel, T. Giessen, K. Jung, H. Ehrhardt, and J. Robertson, Appl. Phys. Lett. **64**, 2797 (1994).
- ³⁰J. Robertson (unpublished).
- ³¹J. Robertson, Philos. Mag. B **66**, 199 (1992).
- ³²N. F. Mott and E. A. Davis, *Electronic Processes in Non-Crystalline Materials* (Oxford University Press, Oxford, 1979).
- ³³J. Ristein, J. Schafer, and L. Ley, Diamond Related Mat. **4**, 508 (1995).